

Sequence analysis

Mutual information without the influence of phylogeny or entropy dramatically improves residue contact prediction

S. D. Dunn¹, L. M. Wahl² and G. B. Gloor^{1,*}¹Department of Biochemistry and ²Department of Applied Mathematics, University of Western Ontario, London, Ontario, Canada, N6A 5C1

Received on October 9, 2007; revised on November 15, 2007; accepted on December 2, 2007

Advance Access publication December 5, 2007

Associate Editor: Alfonso Valencia

ABSTRACT

Motivation: Compensating alterations during the evolution of protein families give rise to coevolving positions that contain important structural and functional information. However, a high background composed of random noise and phylogenetic components interferes with the identification of coevolving positions.

Results: We have developed a rapid, simple and general method based on information theory that accurately estimates the level of background mutual information for each pair of positions in a given protein family. Removal of this background results in a metric, *Mlp*, that correctly identifies substantially more coevolving positions in protein families than any existing method. A significant fraction of these positions coevolve strongly with one or only a few positions. The vast majority of such position pairs are in contact in representative structures. The identification of strongly coevolving position pairs can be used to impose significant structural limitations and should be an important additional constraint for *ab initio* protein folding.

Availability: Alignments and program files can be found in the Supplementary Information.

Contact: ggloor@uwo.ca

Supplementary information: Supplementary data are available at *Bioinformatics* online.

1 INTRODUCTION

In the course of evolution, the amino acid sequences of a family of orthologous proteins slowly change while the fold of the native structure is maintained. Some sequence positions change little, implying that mutations at these sites are not tolerated, and the residues conserved in such positions are inferred to be important for the structure or function of the protein. Sequence positions that vary are expected to be less critical, yet in many cases mutations at these non-conserved positions also cause disruption of structure or loss of function.

How, then, do non-conserved positions change during evolution? It is believed that mutations in these positions can occur because they are either accompanied or preceded by compensatory changes in other variable positions (Fitch *et al.*, 1970; Yanofsky *et al.*, 1964). Such compensation would result in a coupling between changes in the two positions, or

coevolution (Fitch *et al.*, 1970). Since compensation often involves residues that are proximal in the folded structure (Fitch and Markowitz, 1970; Poon and Chao, 2005; Yanofsky *et al.*, 1964), identification of coevolving positions is expected to be useful in the *ab initio* prediction of protein structure from multiple sequence alignments (Fariselli *et al.*, 2001; Gobel *et al.*, 1994; Vendruscolo *et al.*, 1997; Vendruscolo and Domay, 2000).

A number of different approaches to identifying coevolving positions have been developed including methods to detect the differences between observed versus expected frequencies of residue pairs (*OMES*) (Kass and Horovitz, 2002; Larson *et al.*, 2000), the McLachlan Based Substitution correlation (*McBASC*) (Gobel *et al.*, 1994; Olmea *et al.*, 1999), Statistical Coupling Analysis (Lockless and Ranganathan, 1999), Mutual Interdependency (Tillier and Lui, 2003), Coevolution Analysis using Protein Sequence (Fares and Travers, 2006) and Mutual Information (*MI*) based methods (Chiu and Kolodziejczak, 1991; Cover and Thomas, 1991; Korber *et al.*, 1993; Wollenberg and Atchley, 2000). Among these, only the *MI*, *McBASC* and *OMES* methods do not use any structural or phylogenetic information. These methods also do not depend on estimating the significance of coevolution by computationally expensive simulations. A recent study showed that *McBASC* and *OMES* were able to identify contacting pairs better than the *MI* or statistical-coupling methods (Fodor and Aldrich, 2004a).

In the context of multiple sequence alignments, *MI* is an attractive metric because it explicitly measures the dependence of one position on another, but its usefulness has been limited by three factors. First, positions with higher variability, or entropy, will tend to have higher levels of both random and nonrandom *MI* than positions of lower entropy (Fodor and Aldrich, 2004a; Martin *et al.*, 2005), even though the latter are more constrained and would seem more likely to depend on neighboring positions. Second, random *MI* arises because the alignments do not contain enough sequences for background noise to be negligible; our previous modeling studies showed that alignments should contain at least 125 sequences before the random signal begins to subside relative to non-random *MI* (Martin *et al.*, 2005). A third complicating factor is that all position pairs have *MI* due to the phylogenetic relationships of the organisms represented in the alignment

*To whom correspondence should be addressed.

(Wollenberg and Atchley, 2000). This latter source may be limited to some degree by excluding highly similar sequences from closely related species from the alignment, but cannot be eliminated (Martin *et al.*, 2005; Tillier and Lui, 2003). Each of these sources of *MI* will tend to obscure the desired signal based on the structural or functional relationships of positions.

Here we develop a simple method to estimate the expected levels of background *MI* arising from the random and phylogenetic sources. We begin by calculating the *MI* between positions of two different protein families in a *joint alignment* of sequences from the same set of organisms. We find that in the absence of any structural or functional relationships, the *MI* between positions may be estimated with surprising accuracy from the average levels of *MI* observed for those positions in comparison to the average of all joint pairs. Correction of the *MI* values obtained between positions within a protein family by this factor significantly enhances the signal between positions that are close together in the folded protein structure. We further show that the same method can be applied using average *MI* values derived from positions within a single protein family. Since large joint alignments are difficult to produce, this approach is much more accessible. Application of this correction provides a substantial improvement compared to previously published methods for using sequence analysis to find positions that are proximal in the protein structures.

2 APPROACH

Shannon's entropy (*H*) for column *a* in a multiple sequence alignment is a measure of the randomness of the residues in the column (Cover and Thomas, 1991). It is calculated as the sum, over all residues in the column, of the frequency of occurrence of each residue in that column, $p(x, a)$, multiplied by the \log_{20} of that frequency: $H(a) = -\sum_x p(x, a) \log_{20} p(x, a)$. The resulting value varies from 0, in the case of complete conservation, to 1, which occurs when all 20 residues are equally distributed. The observed joint entropy of each pair of positions, $H(a, b)$, is calculated similarly, except di-residue frequencies are used and the sum extends over the possible combinations. The joint entropy values can range from 0 to 2.

MI measures the reduction of uncertainty about one position given information about the other (Cover and Thomas, 1991). This can be thought of as the degree of correlation between two positions *a* and *b* in a multiple sequence alignment. *MI* is calculated $MI(a, b) = H(a) + H(b) - H(a, b)$. *MI* can vary between 0 and 1, with larger values reflecting more interdependence between the positions.

As mentioned above, three factors confound the use of *MI* in identifying covarying positions in protein families. First, *MI* correlates strongly with the entropy of the positions (Fodor and Aldrich, 2004a; Martin *et al.*, 2005). We have previously shown that the influence of entropy can be partially removed by the *MIr* correction (Martin *et al.*, 2005):

$$MIr(a, b) = MI(a, b)/H(a, b). \quad (1)$$

In addition, the *MI* between a pair of positions in a protein family is composed of *MI* due to structural-interactions, functional constraints, random noise and shared ancestry, as

proposed by Wollenburg and Atchley (2000). Thus the challenge is to separate the signal caused by structural and functional constraints, MI_{sf} , from the background, MI_b , which is the sum of contributions from random noise and shared ancestry.

To address this challenge, we postulated that each position in a multiple sequence alignment may have a particular propensity toward MI_b , that is related to its entropy and phylogenetic history, and that the MI_b between any two positions is the product of their propensities. It then follows that MI_b for positions *a* and *b* may be expressed as the product of the average MI_b values of positions *a* and *b* with all other positions in the set, divided by the average MI_b of all positions in the set. We call this term the average product correction, (*APC*), as shown in Equation (5).

In contrast we expected that the *MI* related to structure or function, MI_{sf} , would be highly specific, and for a given position would be found only with a limited number of other positions. Therefore, the difference between the *APC* and total *MI* for a given pair of positions should isolate MI_{sf} . We use MIp to denote this difference, *i.e.*, $MIp(a, b) = MI(a, b) - APC(a, b)$. As illustrated in the Results to follow, a remarkable feature of MIp is that this correction also removes the influence of entropy.

3 METHODS

3.1 The average product correction

To determine the conditions under which the *APC* might closely approximate MI_b , we begin by defining $MI(a, \bar{x})$ as the mean mutual information of column *a*, that is, $MI(a, \bar{x}) = \frac{1}{m} \sum MI(a, x)$, where *n* is the number of columns in the alignment, $m = n - 1$ for convenience, and the summation is over $x=1$ to *n*, $x \neq a$.

Similarly, \bar{MI} denotes the overall mean mutual information, $\bar{MI} = \frac{2}{mn} \sum MI(x, y)$, where the indices run $x=1$ to *m*, $y = x+1$ to *n*.

We also define the mean joint entropy, $H(\bar{x}, \bar{y})$, and the mean joint entropy between a specific column *a* and all other columns, $H(a, \bar{x})$, in the analogous way. Finally, we use \bar{H} to denote the mean entropy of all residues in the alignment.

Expanding the product $MI(a, \bar{x})MI(b, \bar{x})$, we find that it equals:

$$\begin{aligned} & \left(\sum_{x \neq a} MI(a, x) \right) \left(\sum_{x \neq b} MI(b, x) \right) / m^2 \\ &= (mH(a) + \sum_{x \neq a} H(x) - \sum_{x \neq a} H(a, x)) \cdot \\ & \quad (mH(b) + \sum_{x \neq b} H(x) - \sum_{x \neq b} H(b, x)) / m^2 \\ &\approx \bar{H}(H(a) + H(b) - H(a, \bar{x}) - H(b, \bar{x}) + \bar{H}) + \\ & \quad H(a)H(b) - H(a)H(b, \bar{x}) - H(b)H(a, \bar{x}) + H(a, \bar{x})H(b, \bar{x}). \end{aligned} \quad (2)$$

The approximation enters because we have used \bar{H} to approximate both $\sum_{x \neq a} H(x)/m$ and $\sum_{x \neq b} H(x)/m$, which holds for *m* large.

The critical assumption which allows us to proceed further is the following. We assume that the joint entropy contains an additive component from each residue, *i.e.*, that we can approximate $H(a, b)$ as $H(a, b) \approx H(\bar{x}, \bar{y}) + \delta a + \delta b$. Clearly, some δx will be positive and some negative, and by the definition of $H(\bar{x}, \bar{y})$ we find that $\sum_{x=1}^n \delta x = 0$. Thus $\sum_{x \neq a} \delta x = -\delta a$, and we find:

$$\begin{aligned} H(a, \bar{x}) &= H(\bar{x}, \bar{y}) + \delta a - \delta a/m \\ &\approx H(\bar{x}, \bar{y}) + \delta a \end{aligned} \quad (3)$$

since *m* is large.

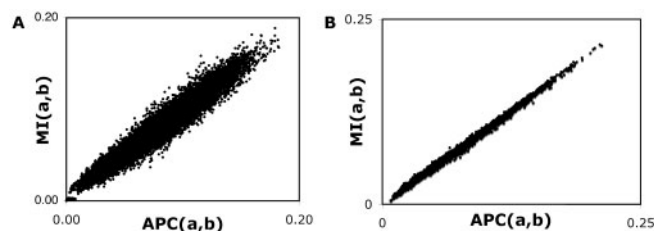


Fig. 1. Scatter plots of the relationships between the *MI* and the *APC* in randomly evolved or in bootstrapped multiple sequence alignments. Panel A shows the relationship found using simulated data that contain random and phylogenetic *MI*. The simulated alignments contained 200 sequences, each with 200 positions, generated by a simple *in silico* evolutionary model, as described in (Martin *et al.*, 2005). Panel B shows that the *APC* closely approximates the mean *MI* from bootstrapped multiple sequence alignments. One hundred multiple sequence alignments that had the same residue frequencies at each position as did the real multiple sequence alignment for GADPH were generated by bootstrapping. The mean *MI* and the resulting *APC* between each pair of positions was calculated. There is an extremely strong relationship ($r = 0.998$). This demonstrates empirically that the *APC* provides an excellent estimation of the background *MI* in alignments without structural or functional information, even for alignments that contain positions with widely varying entropies (H ranges from 0 to 0.85).

Substituting Equation (3) into Equation (2) and using the approximation for $H(a, b)$ to simplify, we find after some manipulation:

$$MI(a, b) \approx \frac{MI(a, \bar{x})MI(b, \bar{x})}{\overline{MI}} - \frac{(H(a) - \bar{H} - \delta a)(H(b) - \bar{H} - \delta b)}{\overline{MI}} \quad (4)$$

The second term on the right will be small if $H(a) \approx \bar{H} + \delta a$, and $H(b) \approx \bar{H} + \delta b$. Empirically, we observe that this equality holds for residues with entropies close to the mean entropy of the alignment, but diverges for small or large entropy residues. Panel A in Figure 1 shows that the first term on the right side (the *APC*) of Equation (4) gives an excellent approximation to $MI(a, b)$ in the absence of structural or functional constraints, for simulated alignments containing random and phylogenetic *MI*. Panel B in Figure 1 shows that the *APC* closely matches the mean *MI* values estimated from bootstrapped multiple sequence alignments.

3.2 The *APC* and *ASC* corrections to *MI*

The rationale described in our Approach, confirmed by the mathematical arguments above, suggest that the average product correction:

$$APC(a, b) = \frac{MI(a, \bar{x})MI(b, \bar{x})}{\overline{MI}} \quad (5)$$

should give an excellent approximation to the background *MI* shared by positions a and b . As stated previously, we use MI_p to denote the difference between total observed *MI* and the *APC*: $MI_p(a, b) = MI(a, b) - APC(a, b)$.

We also explored the possibility that propensities for MI_b were additive rather than multiplicative. This assumption led to the average sum correction:

$$ASC(a, b) = MI(a, \bar{x}) + MI(b, \bar{x}) - \overline{MI}. \quad (6)$$

The difference between the *ASC* and total *MI* is denoted MI_a : $MI_a(a, b) = MI(a, b) - ASC(a, b)$.

3.3 Sequence alignments and structural information

Protein families containing at least 125 independent sequences and at least one solved structure were the same as those used previously (Martin *et al.*, 2005), but were filtered to remove duplicate families and families with only low-resolution structures. A list of the resulting 83 protein families and their alignments are given in Supplementary Table 1. Only ungapped positions in the alignments were considered in our analysis. Residues separated by ≤ 6 Å were defined to be in contact.

3.4 Other covariance measures

An independent method of calculating covariance is to use the sum-of-squares method of Kass and Horovitz, 2002 using the formula:

$$OMES = \frac{-\sum_i^x (N_o - N_e)^2}{N_i} \quad (7)$$

Here, N_o is the observed number of di-aminos in a pair of columns, N_e is the expected number, N is the total number of possible di-amino acid pairs, and N_i is the total number sequences in the alignment. This equation returns the difference between the expected and observed di-amino acid frequencies for a pair of columns. This formula returns 0 if one column or both columns are absolutely conserved, or if the residues in both columns are assorted randomly.

The calculation of *McBASC* is more involved, and was performed as described (Fodor and Aldrich, 2004a) using the software provided by the authors (<http://www.afodor.net/>). Unlike *MI* or *OMES*, *McBASC* returns a high covariance value both for strongly covarying, non-conserved positions, and for highly conserved pairs of positions in a multiple sequence alignment.

3.5 Conversion of *MI* values to Z-scores

We determined how different a given covariance value was relative to all other values in the data set. The mean and SD of the values determined by each of the algorithms were calculated for all pairs of positions. The number of SD from the mean, *i.e.* the Z-score, was determined for each value or for each corrected value in a given data set. Initially, we ensured that the entropy of both positions exceeded 0.3 since previous work showed that positions with an entropy below this value often display *MI* because of insufficient variability (Fodor and Aldrich, 2004a; Martin *et al.*, 2005; Tillier and Lui, 2003). Later analyses were conducted without an entropy cutoff as *MIp* provides an entropy-independent measure. The entropy cutoffs used for each analysis are indicated.

4 RESULTS

4.1 The use of joint alignments of protein families

We made joint alignments of unrelated protein families from the same set of organisms to obtain a data set lacking MI_{sf} . We reasoned that, if most of the proteins are orthologs, the two proteins of a joint alignment should share a similar phylogenetic history since they come from the same organisms. We ignored the possibility of horizontal gene transfer for this analysis. Joint pairs of positions between the two families should have only phylogenetic and random *MI*, *i.e.* MI_b , which is strongly related to the entropy of the positions (Martin *et al.*, 2005). Since the proteins are unrelated and their positions share no MI_{sf} , our starting assumption may be tested by examining the relationship between the *MI* and *APC* values for positions between the protein families.

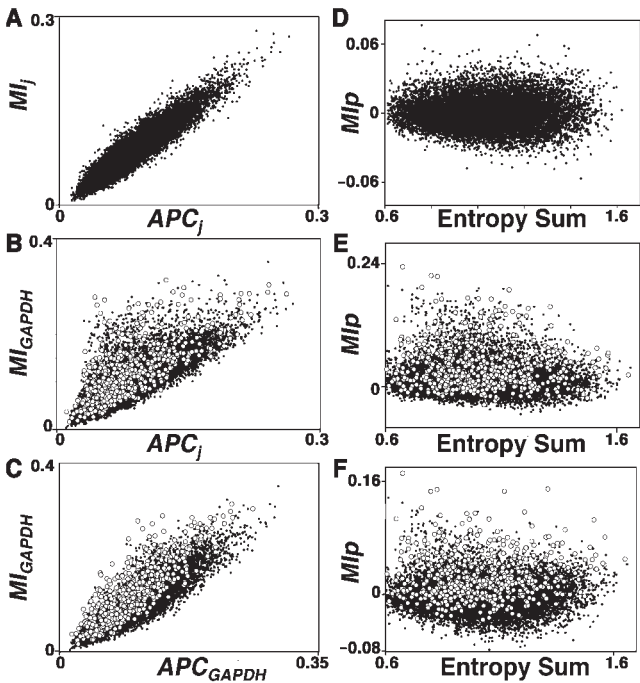


Fig. 2. Scatter plots of the relationships between the *MI* for each pair of positions in a multiple sequence alignment, the *APC* and entropy. Panel A shows the relationship between *MI* and *APC* for the joint pairs of positions in a concatenated GAPDH and NDK multiple sequence alignment. These are labeled MI_j and APC_j . In panel B, *MI* is derived from positions within GAPDH only (MI_{GAPDH}) and is plotted vs. APC_j . In panel C, both *MI* and *APC* were calculated between GAPDH positions. Panels D-F show scatter plots of *MIP* vs. the sum of the entropy for position pairs derived from the same data sets as A-C. These plots show that *MIP*, unlike other measures of coevolution (Fodor and Aldrich, 2004a; Martin *et al.*, 2005), is essentially independent of entropy. The slope of the line of best fit in panel D is 0, in panel E is -0.009 and is 0.0011 in panel F. The open symbols in panels B, C, E and F represent pairs of positions in contact in the representative GAPDH structure 1U8F (Jenkins and Tanner, 2006). Only positions with an entropy of ≥ 0.3 were included in this analysis.

We were able to construct 289 joint alignments from 21 protein families that contained at least 125 unique sequences (chosen from the families in Supplementary Table 1). As a demonstration we show the results for the joint alignment of sequences from 145 organisms for the common enzymes glyceraldehyde 3-phosphate dehydrogenase (GAPDH) and nucleoside diphosphate kinase (NDK). Limiting the analysis to positions with entropy ≥ 0.3 , roughly corresponding to $\leq 70\%$ conservation the GAPDH alignment yielded 165 positions and the NDK alignment yielded 72 positions.

A plot of $MI(a, b)$ between positions of the two proteins in the joint alignment against the *APC* between the positions (Fig. 2A) shows a surprisingly strong and apparently linear relationship. The slope of the line of best fit is 1.0, the *y*-intercept is $1E-6$ and the coefficient of correlation is 0.88. In Figure 2D, the *MIP* values of the joint pairs are plotted as a function of the sum of the entropies of the positions, showing that subtraction of the joint *APC* essentially removes the influence of entropy. Figure 3A shows that the distribution of

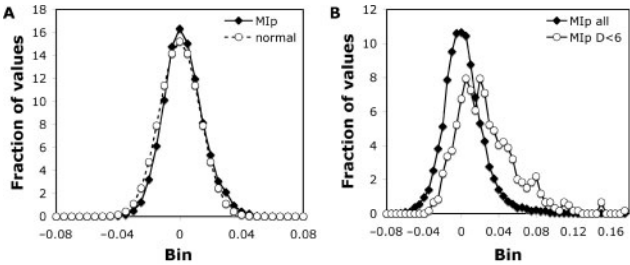


Fig. 3. The distribution of *MIP* values varies depending on the source of the *APC* and *MI* values. *MIP* values were calculated as described in the text and placed into bins of width 0.005. Panel A shows that the frequency of occurrence of values in each of these bins is roughly equally distributed around a mean value of 0 for the joint *MIP* values where both *MI* and *APC* were calculated between pairs of positions in GAPDH and NDK in a concatenated GAPDH and NDK multiple sequence alignment. Panel B shows the distribution of values for GAPDH *MIP* calculated using *MI* and *APC* values derived the GAPDH alignment. The distribution of positions in contact is strongly shifted to the right, and accounts for a substantial fraction of the shoulder and the tail in the overall distribution.

Table 1. The effect of *APC* on *MI*

<i>MI</i> [†] <i>APC</i> [†]	Joint -	Joint Joint	GAPDH -	GAPDH Joint	GAPDH GAPDH
Mean	0.085	0.000	0.100	0.015	0.000
SD	0.038	0.013	0.046	0.029	0.022
Mean Z ($D^* < 6 \text{ \AA}$)	na	na	0.525	0.801	1.082
Median Z ($D < 6 \text{ \AA}$)	na	na	0.370	0.448	0.841
Mean Z ($D > 12 \text{ \AA}$)	na	na	-0.0316	-0.065	-0.094
Median Z ($D > 12 \text{ \AA}$)	na	na	-0.178	-0.241	-0.147

[†]Alignment that is the source of *MI* or *APC* values.

[‡]The minimal distance between non-hydrogen atoms of the residues.

values of *MIP* for the joint pairs is similar to a normal distribution. We infer that the underlying distribution of scores is near normal in the absence of structural or functional relationships between positions.

The average value of *MIP* is 0, and it is notable that the SD of *MIP* for the joint pairs is markedly reduced relative to that for *MI* (Table 1). Since the joint data contain only background *MI*, we interpret this reduction in SD to confirm that the average product correction removes a significant proportion of the background *MI*.

4.1.1 Application of the joint values to GAPDH We next compared the *MI* values between pairs of positions in the GAPDH alignment with *APC* values calculated from the joint alignment (Fig. 2B). The distribution differs from that seen in Figure 2A in that more points are scattered upwards, suggesting that they contain additional *MI* due to structural or functional relationships. This interpretation is supported by the distribution of points representing pairs of positions with minimal inter-residue distances of $\leq 6 \text{ \AA}$ in the GAPDH structure, which are highlighted as open symbols. The SD of *MIP* determined in this way is substantially less than the SD

of *MI* (Table 1). Furthermore, we observe that the mean or the median *MI_p* values for spatially proximal residues are significantly greater than the mean or median *MI* values. These values are expressed as Z-scores (the number of SDs from the mean) in Table 1. Thus *MI_p* calculated by subtraction of the joint *APC* values enhances the signals of many pairs that are expected to have *MI_{sf}* due to proximity.

4.2 Application of intraprotein average *MI* values to correct for *MI_b*

Because of the difficulty of constructing large joint data sets for all proteins of interest, we explored the use of intrafamily values to calculate the *APC* corrections. Most pairs should share only *MI_b* since they are neither proximal nor linked functionally; thus pairs sharing significant *MI_{sf}* should have a small effect on average *MI* values. To test this hypothesis, we calculated the correlation between the position average *MI* values from the joint data sets with position average *MI* values calculated using intraprotein data sets for all protein families in the complete set of 289 joint alignments, using an entropy cutoff of 0.3. The correlation coefficient (*r*) ranged between 0.71 and 0.99 with 256 (88%) of the *r* values being ≥ 0.9 (Supplementary Fig. 1). Interestingly, for 259 of the 289 joint alignments the *r* value was greater than that seen in the GAPDH-NDK joint alignment, which was 0.897. The enzyme SAICAR, which catalyzes a step in purine biosynthesis, was an outlier in this analysis with 15 of the 16 lowest *r* values derived from joint alignments involving this enzyme; indeed, all *r* values below 0.83 were from SAICAR-containing joint alignments. No single protein family predominated at the other end of the distribution. We concluded that the average intraprotein and the average joint *MI* values were strongly related, and inferred that the corresponding joint and intrafamily *APC* corrections were largely equivalent.

In GAPDH, subtraction of intrafamily *APC* to obtain *MI_p* reduced the average value to 0, and again resulted in a major decrease in the standard deviation of the resulting intrafamily *MI_p* values (Table 1). Furthermore, the mean or median Z-scores for spatially proximal pairs of positions were greater than those obtained with *MI_p* derived from the joint alignment. The mean or median Z-scores for residue pairs separated by $\geq 12 \text{ \AA}$ was ≤ 0 (Table 1). The effect of this correction on pairs in contact can be seen clearly by comparing panels A and C in Figure 2. In Figure 3B note that the distribution of *MI_p* scores for pairs in contact is shifted strongly to the right compared to the bulk of the pairs. We conclude that most pairs of positions in contact exhibit coevolution levels ranging from modest to strong as measured by *MI_p*.

4.2.1 Application of intraprotein *MI_p* to multiple protein families

We next compared the ability of intrafamily *MI_p* to identify contacting pairs in a data set of 83 high quality multiple sequence alignments (Methods) to other published methods for finding coevolving positions. First, we measured the fraction of pairs in contact (non-hydrogen atom separations $\leq 6 \text{ \AA}$) as a function of rank order using a variety of methods: *MI*, *MI_r* (Martin *et al.*, 2005), *MI_p*, *MI_a*, *OMES* (Fodor and Aldrich, 2004a) or *McBASC* (Fodor and Aldrich, 2004a). The statistical

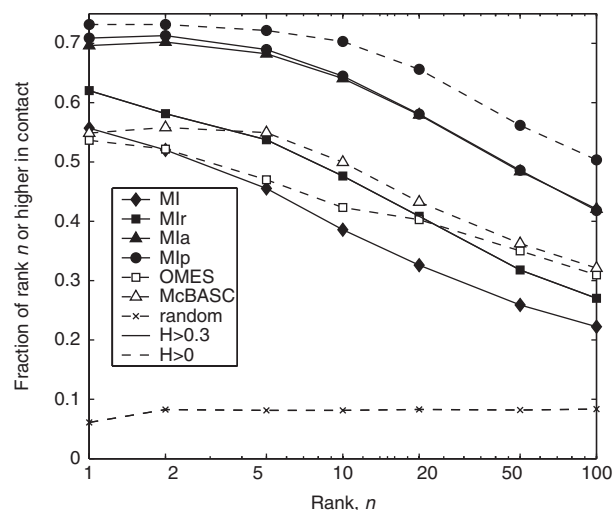


Fig. 4. Plots of the likelihood of contact between pairs of residues in representative structures versus the coevolution ranks for different algorithms. Coevolution between pairs of positions was calculated using either *MI*, *MI_r*, *MI_a*, *MI_p*, *OMES* or *McBASC* across all 83 protein families. Two entropy cutoff values were used in this analysis; 0.3 for the *MI*-based methods, and 0 for *McBASC* and *OMES*. *MI_p* was tested at both entropy cutoffs. For each protein family, the scores from each method were sorted from highest to lowest, the fraction of pairs at each rank or higher that were in contact in a representative structure was tabulated, and averages were plotted. All the methods were significantly better than random chance in identifying contacting pairs. The random line shows the results of a single randomization, the value of which converges to the random contact frequency of 8%.

coupling method was not tested as it is less effective than both *McBASC* and *OMES* (Fodor and Aldrich, 2004a, b). Neither did we test any of the methods that rely on information other than the sequence alignment itself, or any methods that relied on bootstrapping to estimate significance.

In our data set of 83 protein families, each containing at least 125 orthologous members and a representative structure, $\sim 8\%$ of randomly chosen pairs are in contact. Figure 4 shows the proportion of pairs, ranked *n* or higher in each data set that were in contact for each method using either a 0 or 0.3 entropy cutoff as indicated. Among published methods, *MI_r* was best, but none of the methods performed nearly as well as *MI_p* at either entropy cutoff. The *MI_a* method was almost equivalent to *MI_p* in this analysis when an entropy cutoff of 0.3 was used. Interestingly, all of the methods except *MI_p*, *MI_a* and *McBASC* showed a rapid decay versus rank in identifying contacting pairs. In contrast the top five pairs identified by any of these methods were nearly equally likely to be in contact as the top ranked pair of the method.

Finally, we compared each method to find the one that identified the greatest number of contacting pairs in representative structures of the 83 protein family alignments. The pairwise scores from each method were converted to Z-scores and sorted from the highest to lowest score. Single-paired positions are defined as those pairs where each partner had a Z-score above the threshold with only the other residue. In previous work we showed that the residues corresponding to

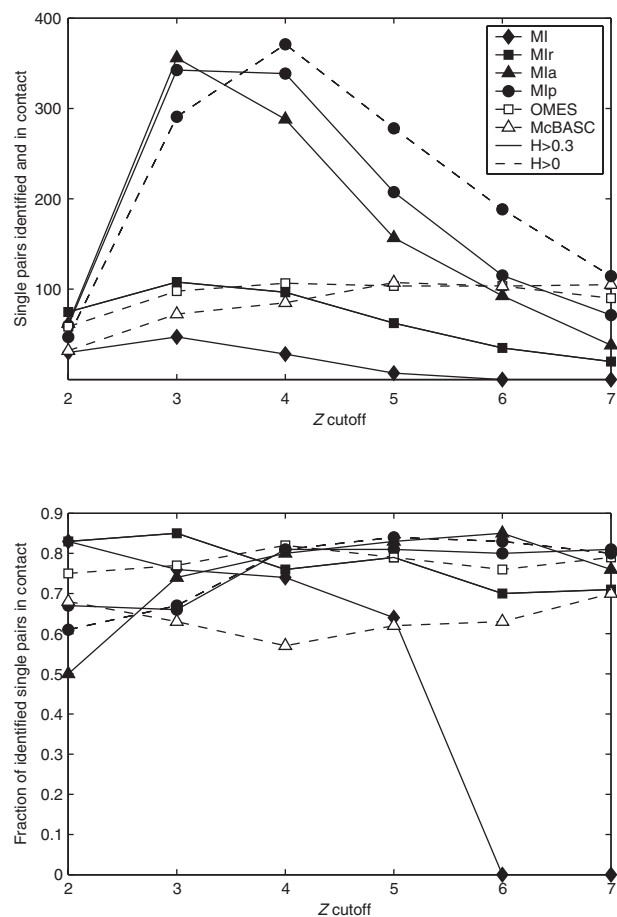


Fig. 5. Plots of the the sensitivity and specificity of the methods at various Z-score cutoff values. The top panel shows the number of single pairs in contact that are found by each method at Z-score cutoffs ranging from 2–7. The bottom panel show the fraction of single pairs identified by each method at each Z-score cutoff which are in contact. The solid lines indicate methods that were evaluated with an entropy cutoff of 0.3, the dashed lines indicate methods evaluated with an entropy cutoff of 0. Data from all 83 protein families were included.

such positions are often found to be in contact if the Z-score threshold was set at 4 (Gloor *et al.*, 2005; Martin *et al.*, 2005). The results of this analysis for each method are shown in Figure 5 and in Supplementary Table 2. We found that all the methods were able to identify a number of pairs in contact with very good accuracy. As expected, *MI* performed the worst, in that this method identified the fewest number of pairs, and in general, the smallest proportion of pairs in contact. Between 75% and 80% of pairs were in contact across a broad range of Z-score cutoffs in the *Mlr*, *OMES*, *Mla* and *Mlp* methods. As expected from the results shown in Figure 4, *Mlp* performed best with an entropy cutoff of 0. Strikingly, *Mlp* uncovered three to four times as many pairs as any other method (other than *Mla*) while maintaining the same accuracy as the other methods (Supplementary Table 2). We conclude that *Mlp* strongly enhances the coevolution score of residues in contact.

4.2.2 Application of intraprotein Mlp to Triosphosphate Isomerase The multiple sequence alignment for the

Table 2. Single pairs in triosephosphate isomerase by each method

pos _i	pos _j	Distance	Mlr [†]	OMES [†]	McBASC [†]	Mlp [‡]
184	227	2.8	7.5	9.1		10.5
142	145	3.1				3.1
179	181	3.1				4.0
216	241	3.1	4.2			7.0
221	224	3.1				4.2
68	70	3.4	5.3			7.9
138	141	3.3	2.1	3.3		5.7
39	246	3.9				3.7
6	9	7.3	4.2			6.0
140	189	4.5				5.0
48	64	4.6			6.2	
135	176	5.6	4.8	5.5	6.7	7.7
209	228	5.6		7.8		
139	186	5.7				5.7
10	235	8.0		2.7		4.9
76	98	8.0 [‡]			10.4	
214	221	8.0			3.2	
9	223	10.2			6.3	
187	219	10.7	4.5			7.5
93	169	11.3		6.1		
187	245	12.7			6.3	
193	231	19.4			5.3	
15	71	23.8 [‡]				3.4
112	178	26.28			9.5	

[†]Z-scores reported with entropy cutoff of 0, except for *Mlr* which had an entropy cutoff of 0.3.

[‡]Pairs in contact across the dimerization interface, intrasubunit distance reported.

homodimeric enzyme triosephosphate isomerase, reported previously (Martin *et al.*, 2005), was used to compare the single pairs identified by each method. Single paired positions at integer Z-score thresholds of 2 through 7 were identified, and positions adjacent in sequence were ignored. Table 2 shows that *Mlr* identified 7 such pairs, five of which were in contact in the structure 1IIH (Noble *et al.*, 1991). Four of these were separated by more than 10 residues in sequence. *Mlp* identified 15 pairs, 11 in intra-subunit contact, and 9 of which were separated by more than 10 residues in sequence. *Mlp* also identified one pair that were far apart within each single subunit, but in contact across the dimerization interface. All the pairs identified by *Mlr* were also found by *Mlp*, in each case with a strikingly higher Z-score. *OMES* identified six pairs, four in contact. *McBASC* found 8 pairs, three of which were in contact including one pair that made contact across the dimer interface. Interestingly, the *OMES*, *McBASC* and *Mlp* methods each found several pairs that the other methods did not, likely because the underlying algorithms are different.

We examined the covariation of one pair corresponding to positions 140–189 in the 1IIH structure. This pair was chosen because it was highly variable in 8 structures derived from different organisms (see Supplementary Tables 3 and 4), and because it was identified only by *Mlp*. As shown in Supplementary Table 3, interactions between these residues comprise a strong ionic interaction, an aromatic ring interaction and various aliphatic interactions. Similar interactions can

be seen among the many common pairs that are found at these positions. We conclude that these positions in the protein family are highly variable, yet must *covary* to maintain a side-chain interaction so that the correct secondary or tertiary structure is maintained.

5 DISCUSSION

A number of obstacles, including random noise, the influence of entropy, the phylogenetic history and the number of sequences required, complicate the identification of coevolving positions in multiple sequence alignments when using *MI* (Martin *et al.*, 2005; Tillier and Lui, 2003). Several groups have used bootstrapping or other randomization methods to attempt to estimate the background coevolution signal (Fares and Travers, 2006; Wollenberg and Atchley, 2000). While bootstrapping can estimate the background due to random noise and the phylogenetic background, the algorithms are computationally expensive and have not been applied to large numbers of protein families. They are also potentially sensitive to our incomplete understanding of the substitution probabilities needed to model the ancestry of the protein family.

We have taken a different approach and developed a correction that rapidly and accurately estimates the background *MI* found in protein family multiple sequence alignments. Our method was initially based on the assumptions that the coevolution signal between pairs of unrelated positions is derived from random noise or from shared ancestry but not from structural or functional constraints; that these factors give each position in an alignment a particular propensity toward MI_b ; that MI_b will be the product of the propensities; and that the gene encoding the protein is inherited as a unit. We have shown that the *APC* accurately estimates *MI* in the absence of structural or functional relationships. Furthermore, in real protein alignments the subtraction of the *APC* from *MI* results in a metric, *MI_p*, that is independent of the entropy of the positions, and that provides a significant improvement over previously published methods in identifying co-evolving positions that are proximal in protein structure.

The *MI_p* metric still requires a significant number of sequences in the protein family because it does not address the finite sample size effects inherent in *MI* (Martin *et al.*, 2005). Supplementary Figure 4 shows that the correct identification of pairs in contact begins to approach the limit when the alignments contain at least 125 non-identical sequences. The exponential growth in the sequence databases, and the availability of sequences from a wide range of organisms enables this requirement to be met for a significant fraction of protein families. Interestingly, as seen in Supplementary Figure 5, the range of variability in the sequences has a smaller effect, so long as the sequences are not identical.

We have also mathematically demonstrated the validity of the *APC* correction. As derived above, the *APC* between two unrelated positions *a* and *b* correctly estimates MI_b if the number of position pairs is large, and if an assumption is made that the joint entropy is composed of an additive component from each individual position. The *MI_p* values deviate somewhat when the position entropy and the mean entropy are

different, but this results in errors in the *Z*-scores of ≤ 0.2 when 50 or more positions are used for the calculation, and falls to ≤ 0.1 when the number of positions is ≥ 100 (Supplementary Fig. 2). These deviations are consistent with the algebraic modeling, and are much less than that observed for either *MI* or *MI_r* (Supplementary Fig. 2). Furthermore, modeled coevolving positions in protein families shows that *MI_p* is significantly more sensitive and more selective than other methods (Supplementary Fig. 3). Since the *APC* is an accurate estimate of the background *MI*, we conclude that the residual *MI_p* is an accurate estimate of the coevolution signal caused by structural and functional correlations, MI_{sf} .

The *ASC* correction performed nearly as well as the *APC* correction in improving the coevolution signal between proximal residues. This result implies that the largest error in application of either correction is not related to whether the correction provides the most probable level of MI_b for the data set, but rather whether the data set itself is large enough that observed levels of *MI* are likely to approach the most probable levels. Once again, it is beneficial to have as many sequences in the alignment as possible, which can be achieved using the intrafamily *APC* values, since joint alignments will usually contain fewer sequences.

Even when the intrafamily alignments were restricted to those in the joint alignments, however, we found that the intrafamily *MI_p* gave lower SD and thus higher *Z*-scores for proximal positions in comparison to the joint *MI_p*. Two factors may contribute to these effects. First, we and others have previously shown that positions with high *MI* can be divided into group coevolvers, which appear to coevolve with multiple positions and are often not in contact, and isolated pairs, which are in contact and coevolve strongly with each other only (Fares and Travers, 2006; Gloor *et al.*, 2005; Martin *et al.*, 2005). The intrafamily *APC* correction, but not the joint *APC* correction, may tend to suppress the signals from the group coevolvers, since their average *MI* will be elevated relative to other positions of similar entropy, and this could lead to a tightening of the residual intrafamily *MI_p* values. The net effect of this would be to enhance the *Z*-scores of the isolated pairs. Second, the possible presence of entire genes acquired through lateral transfer will affect the validity of the joint *APC* correction but not the intrafamily *APC* correction, since the latter requires only that genes were inherited as units.

Interestingly, the right side of the intrafamily *MI_p* distribution shown in Figure 3 has both a shoulder and a tail, and the positions in contact have a significantly different distribution than the bulk of the pairs. These observations suggest that, while a small number of important contacting pairs share high MI_{sf} , there are many more pairs with lower levels of MI_{sf} that may also contribute to protein structure or function. We have found that position pairs with lower amounts of MI_{sf} show strong correlations with local and long-distance secondary structure (in preparation), and are currently working to incorporate these constraints to further use MI_{sf} to aid in *de novo* protein folding.

We also noted that within the GAPDH tetrameric structure, positions in contact between subunits had substantially higher average and median *MI_p* than those in contact within a subunit. Furthermore, *MI_p* can be applied to membrane

proteins where it has been used to identify key coevolving residues that allowed the identification of structural and functional signals in the Major Intrinsic Protein family of membrane proteins (Arinaminpathy, Gloor, Gerstein and Engelman, submitted for publication). Together with the identification of the intersubunit contact of positions 15 and 71 in triosephosphate isomerase (Table 2), these preliminary observations imply that *Mip* can identify proximal positions across subunit interfaces, and may lead to methods to identify interacting protein partners.

6 CONCLUSION

We have found that the background *MI* of each pair of positions in a multiple sequence alignment can be accurately estimated from mean *MI* values of each position. We have shown that the resulting value, the *APC*, accurately estimates the background *MI* provided the number of positions in the protein family is equal to or greater than the size of a typical protein domain. This measure can be rapidly calculated from the *MI* values for a multiple sequence alignment. Subtraction of the *APC* from the *MI* produces a new covariance measure which we term *Mip*. The *Mip* is substantially more sensitive and selective than previous methods at finding pairs of positions in contact in real protein families.

ACKNOWLEDGEMENTS

The authors would like to acknowledge the insightful comments of two anonymous reviewers. Work in the labs of S.D.D. and G.B.G. is supported by operating grants from the Canadian Institutes of Health Research. Work by L.M.W. is supported by the National Science and Engineering Research Council of Canada, and by the Canada Research Chairs program.

Conflict of Interest: none declared.

REFERENCES

- Chiu, D.K. and Kolodziejczak, T. (1991) Inferring consensus structure from nucleic acid sequences. *Comput. Appl. Biosci.*, **7**, 347–52.
- Cover, T.M. and Thomas, J.A. (1991) *Elements of information theory*. Wiley, New York.
- Cuff, J.A. et al. (1998) JPred: a consensus secondary structure prediction server. *Bioinformatics*, **14**, 892–3.
- Fares, M.A. and Travers, S.A. (2006) A novel method for detecting intramolecular coevolution: adding a further dimension to selective constraints analyses. *Genetics*, **173**, 9–23.
- Fariselli, P. et al. (2001) Progress in predicting inter-residue contacts of proteins with neural networks and correlated mutations. *Proteins*, **S5**, 157–162.
- Fitch, W.M. and Markowitz, E. (1970) An improved method for determining codon variability in a gene and its application to the rate of fixation of mutations in evolution. *Biochem. Genet.*, **4**, 579–593.
- Fodor, A.A. and Aldrich, R.W. (2004a) Influence of conservation on calculations of amino acid covariance in multiple sequence alignments. *Proteins*, **56**, 211–221.
- Fodor, A.A. and Aldrich, R.W. (2004b) On evolutionary conservation of thermodynamic coupling in proteins. *J. Biol. Chem.*, **279**, 19046–19050.
- Gloor, G. et al. (2005) Information in protein multiple sequenced alignments reveals two classes of coevolving positions. *Biochemistry*, **44**, 7156–7165.
- Gobel, U. et al. (1994) Correlated mutations and residue contacts in proteins. *Proteins*, **18**, 309–317.
- Jenkins, J.L. and Tanner, J.J. (2006) High-resolution structure of human D-glyceraldehyde-3-phosphate dehydrogenase. *Acta Crystallogr. D Biol. Crystallogr.*, **62**, 290–301.
- Kass, I. and Horovitz, A. (2002) Mapping pathways of allosteric communication in GroEL by analysis of correlated mutations. *Proteins*, **48**, 611–617.
- Korber, B.T. et al. (1993) Covariation of mutations in the V3 loop of human immunodeficiency virus type 1 envelope protein: an information theoretic analysis. *Proc. Natl Acad. Sci. USA*, **90**, 7176–80.
- Larson, S.M. et al. (2000) Analysis of covariation in an SH3 domain sequence alignment: applications in tertiary contact prediction and the design of compensating hydrophobic core substitutions. *J. Mol. Biol.*, **303**, 433–446.
- Lockless, S.W. and Ranganathan, R. (1999) Evolutionarily conserved pathways of energetic connectivity in protein families. *Science*, **286**, 295–299.
- Martin, L.C. et al. (2005) Using information theory to search for co-evolving residues in proteins. *Bioinformatics*, **21**, 4116–4124.
- Noble, M.E. et al. (1991) The adaptability of the active site of trypanosomal triosephosphate isomerase as observed in the crystal structures of three different complexes. *Proteins*, **10**, 5069.
- Olmea, O. et al. (1999) Effective use of sequence correlation and conservation in fold recognition. *J. Mol. Biol.*, **293**, 1221–1239.
- Poon, A. and Chao, L. (2005) The rate of compensatory mutation in the DNA bacteriophage ϕ X174. *Genetics*, **170**, 989–999.
- Tillier, E.R. and Lui, T.W. (2003) Using multiple interdependency to separate functional from phylogenetic correlations in protein alignments. *Bioinformatics*, **19**, 750–755.
- Vendruscolo, M. et al. (1997) Recovery of protein structure from contact maps. *Fold. Des.*, **2**, 295–306.
- Vendruscolo, M. and Domany, E. (2000) Protein folding using contact maps. *Vitam. Horm.*, **58**, 171–212.
- Wollenberg, K.R. and Atchley, W.R. (2000) Separation of phylogenetic and functional associations in biological sequences by using the parametric bootstrap. *Proc. Natl Acad. Sci. USA*, **97**, 3288–3291.
- Yanofsky, C. et al. (1964) Protein Structure Relationships Revealed by Mutational Analysis. *Science*, **146**, 1593–1594.